Article

Discovery Medicine 2025; 37(200): 1896–1913
https://doi.org/10.24976/Discov.Med.202537200.164

Galectin-3 Preserves Intestinal Barrier Function via Regulation of the JAK2/STAT3 Signaling Pathway During Ischemia-Reperfusion Injury in Mice

Weilai Yu[1], Zhixiang Lin[1], Liwei Xue[1], Qiu Chen[2], Siwei Xue[3,*]

[1]Department of Gastroenterology, The Third Affiliated Hospital of Wenzhou Medical University, 325200 Wenzhou, Zhejiang, China
[2]Department of Endocrinology, The Third Affiliated Hospital of Wenzhou Medical University, 325200 Wenzhou, Zhejiang, China
[3]Department of Gastroenterology, The People's Hospital of CangNan, 325800 Wenzhou, Zhejiang, China
*Correspondence: 2008xsw@163.com (Siwei Xue)
Submitted: 25 July 2025 Revised: 12 August 2025 Accepted: 26 August 2025 Published: 20 September 2025

Background: Intestinal ischemia-reperfusion injury (IRI) is a severe complication of major surgeries and shock, leading to intestinal barrier dysfunction and systemic inflammation. Treatment options remain limited due to poorly defined mechanisms. Galectin-3, a β-galactoside-binding lectin that regulates inflammatory processes, has emerged as a potential modulator of tissue injury. This study aimed to investigate the role of Galectin-3 in IRI, focusing on janus kinase 2/signal transducer and activator of transcription 3 (JAK2/STAT3) regulation to identify potential therapeutic targets.

Methods: After establishing a murine intestinal IRI model, mice were treated with varying doses of G3-C12, a Galectin-3 inhibitor. Intestinal injury, inflammation, tight junction protein (TJP) expression, apoptosis, and JAK2/STAT3 pathway activation were assessed using hematoxylin-eosin (H&E) staining, quantitative real-time polymerase chain reaction (qRT-PCR), Western blotting, terminal deoxynucleotidyl transferase dUTP nick-end labeling (TUNEL) assay, and caspase activity assays. Additionally, the Caco-2 oxygen-glucose deprivation/reoxygenation (OGD/R) model was employed to validate the mechanism of Galectin-3, with pathway dependency evaluated using the JAK2 agonist C-A1.

Results: IRI induced significant intestinal structural disruption, increased pro-inflammatory cytokines (interleukin-6 [IL-6], tumor necrosis factor-α [TNF-α], $p < 0.001$), reduced anti-inflammatory interleukin-10 (IL-10) ($p < 0.001$), downregulated TJPs ($p < 0.001$), and elevated apoptosis ($p < 0.001$) in mice. These alterations coincided with upregulation of Galectin-3, phosphorylated JAK2 (p-JAK2), and phosphorylated STAT3 (p-STAT3) ($p < 0.001$). G3-C12 treatment markedly alleviated histopathological injury, reduced inflammation and apoptosis, dose-dependently restored TJP expression, and suppressed JAK2/STAT3 pathway activation ($p < 0.01$ or $p < 0.001$). *In vitro* OGD/R assays further demonstrated that G3-C12 improved cell viability, reduced lactate dehydrogenase (LDH) release, attenuated inflammation and apoptosis, and restored TJP levels, effects that were partially reversed by JAK2 activation with C-A1.

Conclusion: Galectin-3 is upregulated during IRI and promotes JAK2/STAT3 pathway activation, exacerbating inflammation and intestinal barrier dysfunction. Inhibition of Galectin-3 suppresses this aberrant signaling, mitigates intestinal injury, reduces apoptosis and inflammation, and restores TJPs expression and mucosal barrier integrity. These findings suggest Galectin-3 as a promising therapeutic target for IRI.

Keywords: intestinal ischemia-reperfusion injury; Galectin-3; JAK2/STAT3 signaling pathway; intestinal mucosal barrier; inflammation

Introduction

Intestinal ischemia-reperfusion injury (IRI) is a common and severe pathological condition characterized by complex mechanisms involving dysregulation and excessive activation of multiple signaling pathways [1]. During IRI, diverse pathological mechanisms, including inflammation, oxidative stress, impaired autophagy, and aberrant macrophage polarization, contribute to the structural integrity and normal function of the intestinal mucosal barrier [2,3]. Damage to this barrier increases intestinal permeability, allowing the translocation of bacteria, endotoxins, and inflammatory mediators into the bloodstream, potentially initiating systemic inflammatory response syndrome (SIRS) and multiple organ dysfunction syndrome (MODS) [4,5]. Therefore, identifying effective strategies to preserve mucosal barrier integrity is critical for the prevention and management of IRI.

The intestinal mucosal barrier serves as an essential biological defense system that prevents luminal bacteria and endotoxins from entering the host, and is composed of three principal components: mechanical, biological, and immune barriers [6,7]. Among these, the immune barrier is especially vital for host protection against infections and for reg-

ulating inflammatory homeostasis [8]. However, IRI frequently causes barrier breakdown, enabling luminal contents to translocate into the bloodstream and initiating a vicious inflammatory cycle that exacerbates systemic injury.

Galectin-3, a β-galactoside-binding lectin encoded by the galectin gene family, is widely expressed in macrophages, epithelial cells, cardiovascular tissues, and immune cells [9]. Recent evidence demonstrates that Galectin-3 plays a critical role in diverse ischemia-reperfusion (IR) injury models by modulating inflammation, oxidative stress, programmed cell death, autophagy, and fibrotic remodeling via multiple signaling cascades and cellular mechanisms [10–12]. Within inflammatory responses, Galectin-3 modulates immune cell activity and alters cytokine secretion profiles, which include both pro- and anti-inflammatory mediators, thereby influencing the initiation, progression, and resolution of inflammation [13]. However, the precise mechanisms by which Galectin-3 regulates the structural stability of the intestinal mucosal barrier during IRI remain unclear.

The janus kinase (JAK)/signal transducer and activator of transcription (STAT) signaling pathway is a key regulator of cellular processes, including proliferation, differentiation, apoptosis, and immune regulation [14,15]. In particular, the JAK2/STAT3 axis plays a pivotal role in mediating inflammatory responses and tissue repair following ischemia-reperfusion injury [16,17]. Activation of this pathway governs the production of major effector molecules, including interleukin-6 (IL-6), tumor necrosis factor-α (TNF-α), and interleukin-10 (IL-10), which act as both pro- and anti-inflammatory mediators, thereby exerting dual roles in the pathophysiology of IR injury [18]. The JAK2/STAT3 pathway is also essential in intestinal homeostasis and inflammatory bowel diseases by modulating T cell survival, proliferation, and differentiation, as well as antiviral responses and B cell activity, thereby influencing barrier function and immune regulation [19]. However, it remains uncertain whether Galectin-3 exerts its protective effect on the intestinal barrier through JAK2/STAT3 signaling during IRI.

In this study, we established a murine model of intestinal IRI together with an *in vitro* oxygen-glucose deprivation/reoxygenation (OGD/R) model to investigate the role of Galectin-3 in regulating the intestinal mucosal barrier under IRI conditions. Furthermore, we examined the involvement of the JAK2/STAT3 signaling pathway in this process. Our objective was to elucidate the protective mechanisms mediated by Galectin-3, expand current knowledge of IRI pathophysiology, and propose new theoretical insights and potential therapeutic targets for the clinical management of IRI.

Materials and Methods

Experimental Animals

Forty male C57BL/6 specific pathogen-free (SPF) mice, aged 8–10 weeks and weighing 25.0 $\pm$ 3.0 g, were obtained from SPF Biotechnology Co., Ltd. (Beijing, China) under license SCXK (Jing) 2019-0010. The animals were housed under standard conditions with *ad libitum* access to food and water. Following a 7-day acclimatization period, experimental procedures were initiated. All animals conformed to the health standards for conventional laboratory animals in China.

Establishment of Mouse IRI Model

After acclimation for seven days, mice were randomly allocated into the following groups: sham-operated control (Sham), ischemia-reperfusion injury (IRI), and Galectin-3 inhibitor (G3-C12) intervention groups at low, medium, and high doses (1.0, 2.5, and 5.0 mg/kg) [20], with 8 animals per group. For three consecutive days before IRI induction, mice in the intervention groups received daily tail vein injections of G3-C12 (HY-P1592, MedChem Express, Monmouth Junction, NJ, USA) at the designated doses, dissolved in normal saline (ST341, Beyotime, Shanghai, China). Control animals received equivalent volumes of saline. Prior to surgery, mice were fasted for 12 hours with unlimited access to water. Anesthesia was induced with 2–3% isoflurane in a specialized chamber and maintained at 1.5–2% isoflurane via a nasal cone throughout the surgical intervention. Following the protocol described previously [21], IRI was induced by occluding the superior mesenteric artery (SMA) with a vascular clamp for 45 minutes, followed by 120 minutes of reperfusion after clamp removal. In the Sham group, the SMA was exposed but not clamped. Vital signs were continuously monitored throughout the procedure. Upon completion of the 120-minute reperfusion, mice were deeply anesthetized with intraperitoneal pentobarbital sodium (100 mg/kg; P3761, Think-Far, Beijing, China) and euthanized. Blood and intestinal tissues were immediately collected for subsequent analyses.

Cell Culture and Treatment

The Caco-2 cell line (human colorectal adenocarcinoma, JNO-H0110) was purchased from Geneo BioTech Co., Ltd. (Guangzhou, China). Cells were cultured in RPMI-1640 culture medium (G4531, Servicebio, Wuhan, China) supplemented with 10% fetal bovine serum (SNS-001, SUNNCELL, Wuhan, China) and 50 mg/L penicillin/streptomycin (GNM15140-1, GENOM-BIO, Hangzhou, China), under standard conditions (37 °C, 5% CO_2, and 95% air). Short tandem repeat analysis was used for authentication, and all cultures were confirmed to be mycoplasma-free.

An OGD/R model was established in Caco-2 cells as previously described [21]. Briefly, Caco-2 cells were cul-

tured in glucose-free medium (G4538, Servicebio, Wuhan, China) and exposed to hypoxic conditions (94% N_2, 4% CO_2, and 1% O_2) for 12 hours. Cells were then reoxygenated under normoxic conditions (95% air, 5% CO_2) for 4 hours. Experimental groups included: Control, OGD/R, JAK2 agonist (coumermycin A1, C-A1), Galectin-3 inhibitor (G3-C12), and combined Galectin-3 inhibitor plus JAK2 agonist (G3-C12 + C-A1). One hour prior to OGD/R exposure, cells in the G3-C12 group were pretreated with G3-C12 (50 µM), while the G3-C12 + C-A1 group received a combination of G3-C12 (50 µM) and JAK2 agonist C-A1 (10 µM, HY-N7452, MedChem Express, NJ, USA). Except for the Control group, all groups received equivalent volumes of vehicle at corresponding time points as controls. Following the 4-hour reoxygenation phase, cell pellets and culture supernatants were harvested for downstream experimental analyses.

Histopathological Examination of Intestinal Tissue

Intestinal tissues were collected and fixed in 4% paraformaldehyde solution (P0099, Beyotime, Shanghai, China) for 24 hours. After dehydration, clearing, paraffin embedding, and sectioning, tissue slices were prepared. The sections were stained with hematoxylin-eosin (H&E, G1076, Servicebio, Wuhan, China), and morphological changes of the intestinal mucosa were examined using a light microscope (Leica DM2000, Leica, Wetzlar, Germany).

Detection of Inflammatory Cytokines and Intestinal Injury Markers

Following model induction, mice were anesthetized for blood collection. After a 10-minute incubation at room temperature, samples were centrifuged (3000 rpm, 10 min, 4 °C) to isolate serum. The terminal ileum was excised, weighed, and homogenized in ice-cold phosphate-buffered saline (PBS) (C0221A, Beyotime) at a tissue-to-volume ratio of 1:9 (mg:µL) to yield 10% homogenates. The homogenates were centrifuged (3000 rpm, 10 min, 4 °C), and supernatants were collected for testing. Enzyme-linked immunosorbent assay (ELISA) kits were used to measure IL-6, TNF-α, and IL-10 levels in intestinal tissues (SEKM-0007, SEKM-0034, SEKM-0010; Solarbio, Beijing, China); D-lactate and intestinal fatty acid-binding protein (I-FABP) in serum (ML-sa-7434, S0204S, ELISA-00801; MeiLianShengWu, Shanghai, China); and the endothelial injury marker Syndecan-1 (JLC2769, Gelatins, Shanghai, China), following manufacturers' protocols.

Cell Viability Assay

Caco-2 cells (1×10^5/well) were seeded in 96-well plates and then subjected to the indicated treatments. Consequently, 10 µL of Cell Counting Kit-8 (CCK-8, C0037, Beyotime, Shanghai, China) reagent was added to each well and incubated at 37 °C for 1–2 hours. Absorbance at 450 nm was recorded using a microplate reader (CMaxPlus, Molecular Devices, San Jose, CA, USA).

Cell Death Assay

Cell death was quantified by measuring lactate dehydrogenase (LDH) release from Caco-2 cells cultured in 96-well plates and then subjected to the indicated treatments. LDH activity was assessed using a commercial kit (CB11219, COIBO BIO, Shanghai, China) following the manufacturer's instructions.

Measurement of Inflammatory Cytokines in Cells

Levels of IL-6, TNF-α, and IL-10 in Caco-2 supernatants were quantified using ELISA kits (SEKH-0013, SEKH-0047, SEKH-0018; Solarbio, Beijing, China) according to the manufacturer's instructions.

Caspase Activity Assay

To assess apoptosis-related activity, caspase-3 and caspase-9 enzyme functions were determined using dedicated assay kits (BC3830, BC3890; Solarbio, Beijing, China). Intestinal homogenates were prepared as previously described, while Caco-2 cells were lysed in kit buffer and centrifuged. Substrates were added to the supernatants and incubated at 37 °C, after which absorbance was measured at 405 nm using a microplate reader (CMaxPlus, Molecular Devices, San Jose, CA, USA).

TUNEL Assay for Apoptosis Detection

Apoptosis in intestinal tissues and Caco-2 cells was detected using a terminal deoxynucleotidyl transferase dUTP nick-end labeling (TUNEL) assay kit (MA0224, Meilunbio, Dalian, China). Paraffin-embedded intestinal tissue sections were deparaffinized, rehydrated, and digested with proteinase K (37 °C, 15 min). Cells were fixed with 4% paraformaldehyde for 30 minutes, washed with PBS. For nuclear staining, 4′,6-diamidino-2-phenylindole (DAPI C1006, Beyotime, Shanghai, China) was applied according to the manufacturer's instructions. TUNEL staining was performed following the kit protocol. Images were captured with an Olympus CX41 fluorescence microscope (CX41-32RFL, Olympus, Tokyo, Japan), and TUNEL-positive cells were quantified using ImageJ software (v1.46; National Institutes of Health, Bethesda, MD, USA).

Quantitative Real-Time Polymerase Chain Reaction (qRT-PCR)

Total RNA was extracted from intestinal tissues and Caco-2 cells using TRIzol (abs60154, Absin, Shanghai, China). Complementary DNA (cDNA) was synthesized with the microRNA (miRNA) 1st Strand cDNA Kit (MR201-01, Vazyme, Nanjing, China). qRT-PCR was conducted on QuantStudio 5 (Applied Biosystems, Foster City, CA, USA) using the HiScript II One Step

qRT-PCR SYBR Green Kit (Q221-01, Vazyme, Nanjing, China). Glyceraldehyde-3-phosphate dehydrogenase (GAPDH) served as the internal control, and relative expression was calculated by the $2^{-\Delta\Delta CT}$ method. Primer sequences are listed in Table 1.

Western Blotting (WB)

Proteins were extracted from intestinal tissues and Caco-2 cells using radio-immunoprecipitation assay buffer (20101ES60, YEASEN, Shanghai, China). Following protein quantification, samples were separated by sodium dodecyl sulfate-polyacrylamide gel electrophoresis and transferred onto polyvinylidene difluoride membranes. Membranes were blocked with 5% non-fat milk for 1 hour and incubated overnight at 4 °C with primary antibodies against Galectin-3, zonula occludens-1 (ZO-1), occludin, claudin-1, and hypoxia-inducible factor 1 alpha (HIF-1α) (14979-1-AP, 21773-1-AP, 27260-1-AP, 28674-1-AP, 20960-1-AP; Proteintech, Wuhan, China); phosphorylated JAK2 (p-JAK2), JAK2, phosphorylated STAT3 (p-STAT3), and STAT3 (3771, 3230, 9145, 30835; Cell Signaling Technology, MA, USA); and GAPDH (GB11002-100, Servicebio, Wuhan, China) served as the internal control. Membranes were then incubated with HRP-conjugated goat anti-rabbit secondary antibodies (A0208, Beyotime, Shanghai, China) for 60 minutes. Protein expression was normalized to GAPDH, and bands were visualized by chemiluminescence (Bio-Rad Laboratories, Hercules, CA, USA) and quantified using ImageJ software (v1.46; National Institutes of Health, Bethesda, MD, USA).

Statistical Analysis

Statistical analyses were performed using GraphPad Prism 9.5 (GraphPad Software, San Diego, CA, USA). Comparisons between two groups were conducted with Student's *t*-test, while multiple groups were analyzed using one-way ANOVA followed by Tukey's post hoc test after confirming normality, variance homogeneity, and independence. Corrections for multiple testing were applied where appropriate. Data are presented as mean $\pm$ standard deviation (SD), and $p < 0.05$ was considered statistically significant.

Results

Galectin-3 Inhibition Attenuates IRI-Induced Intestinal Inflammation and Improves Mucosal Barrier Function

Serum intestinal injury biomarkers revealed that levels of D-lactate, I-FABP, and Syndecan-1 were significantly elevated in the IRI group compared to Sham controls ($p < 0.001$), indicating that IRI induces marked injury to the intestinal mucosa and vascular endothelium. Following treatment with increasing doses of G3-C12, these biomarkers declined in a dose-dependent manner, with the greatest reduction observed in the high dose group (G3-C12-H, 5.0 mg/kg) ($p < 0.001$) (Fig. 1A). These findings suggest that Galectin-3 inhibition effectively alleviates IRI-induced intestinal injury and improves barrier function.

Inflammatory cytokine expression of IL-6, TNF-α, and IL-10 in intestinal tissues was evaluated by ELISA and qRT-PCR. The IRI group demonstrated markedly elevated IL-6 and TNF-α expression and significantly reduced IL-10 compared to the Sham group ($p < 0.001$) (Fig. 1B,C). Administration of G3-C12 significantly attenuated inflammation, as shown by reduced IL-6 and TNF-α levels ($p < 0.01$ or $p < 0.001$) and increased IL-10 expression ($p < 0.01$ or $p < 0.001$). The most pronounced effect was observed in the high-dose group. Collectively, these findings indicate that Galectin-3 inhibition mitigates mucosal injury and inflammatory responses, thereby improving intestinal permeability and reducing tissue damage.

Inhibition of Galectin-3 Ameliorates Intestinal Mucosal Architecture and Tight Junction Proteins (TJPs) Expression in IRI Mice

H&E staining revealed that intestinal tissue from the Sham group exhibited intact architecture, with well-organized villi and no visible injury. Conversely, the IRI group exhibited substantial histological abnormalities, including villus detachment, epithelial cell necrosis, lamina propria edema, and inflammatory cell infiltration. Treatment with various doses of the Galectin-3 inhibitor G3-C12 markedly alleviated these pathological changes, characterized by more intact villus architecture and reduced inflammatory infiltration. The extent of improvement correlated with the administered dose, with maximal efficacy observed in the high-dose group (Fig. 2A).

WB analysis demonstrated a significant decline in TJP expression in the IRI-treated samples compared to the Sham controls ($p < 0.001$). G3-C12 treatment restored protein levels in a dose-dependent manner, with significant increases at medium and high doses ($p < 0.05$, $p < 0.01$ or $p < 0.001$) (Fig. 2B,C). Similarly, qRT-PCR analysis demonstrated that mRNA levels of TJPs were significantly downregulated in the IRI group versus the Sham group ($p < 0.001$), whereas G3-C12 administration significantly upregulated their expression, particularly in the high-dose group ($p < 0.001$) (Fig. 2D). Collectively, the results indicate that Galectin-3 inhibition significantly mitigates IRI-induced histopathological damage and promotes the recovery of intestinal mucosal barrier integrity by upregulating the expression of TJP.

Galectin-3 Inhibition Attenuates Intestinal Epithelial Cell Apoptosis in IRI Mice

TUNEL staining revealed a notable increase in apoptotic cells within the intestinal tissues of the IRI group compared to the Sham group ($p < 0.001$), evidenced by a significantly higher number of TUNEL-positive cells.

Table 1. Primer sequences used for qRT-PCR analysis.

Gene name	Species	Primer sequence (5′-3′)
IL-6	Human	F: AGACAGCCACTCACCTCTTCAG
		R: TTCTGCCAGTGCCTCTTTGCTG
IL-6	Mouse	F: TACCACTTCACAAGTCGGAGGC
		R: CTGCAAGTGCATCATCGTTGTTC
TNF-α	Human	F: AGGGTCTGGGCCATAGAACT
		R: CCACCACGCTCTTCTGTCTAC
TNF-α	Mouse	F: AAGCCTGTAGCCCACGTCGTA
		R: GGCACCACTAGTTGGTTGTCTTTG
IL-10	Human	F: TCTCCGAGATGCCTTCAGCAGA
		R: TCAGACAAGGCTTGGCAACCCA
IL-10	Mouse	F: CGGGAAGACAATAACTGCACCC
		R: CGGTTAGCAGTATGTTGTCCAGC
ZO-1	Human	F: GTCCAGAATCTCGGAAAAGTGCC
		R: CTTTCAGCGCACCATACCAACC
ZO-1	Mouse	F: GTTGGTACGGTGCCCTGAAAGA
		R: GCTGACAGGTAGGACAGACGAT
Occludin	Human	F: ATGGCAAAGTGAATGACAAGCGG
		R: CTGTAACGAGGCTGCCTGAAGT
Occludin	Mouse	F: TGGCAAGCGATCATACCCAGAG
		R: CTGCCTGAAGTCATCCACACTC
Claudin-1	Human	F: GGATCCATGGCCAACGCGGGGCT
		R: AAGCTTTCACACGTAGTCTTTCCCG
Claudin-1	Mouse	F: GCTGGGTTTCATCCTGGCTTCT
		R: CCTGAGCGGTCACGATGTTGTC
JAK2	Human	F: CCAGATGGAAACTGTTCGCTCAG
		R: GAGGTTGGTACATCAGAAACACC
JAK2	Mouse	F: GCTACCAGATGGAAACTGTGCG
		R: GCCTCTGTAATGTTGGTGAGATC
STAT3	Human	F: CTTTGAGACCGAGGTGTATCACC
		R: GGTCAGCATGTTGTACCACAGG
STAT3	Mouse	F: AGGAGTCTAACAACGGCAGCCT
		R: GTGGTACACCTCAGTCTCGAAG
Galectin-3	Human	F: GCTGGGCCACTGATTGTGC
		R: CTGTTTGCATTGGGCTTCAC
Galectin-3	Mouse	F: ACGCCATGATCTAAGCCAGA
		R: GCGATGGGTATCTCTCAGCC
HIF-1α	Human	F: TGGCTGCATCTCGAGACTTT
		R: GAAGACATCGCGGGGAC
GAPDH	Human	F: ATGGGGAAGGTGAAGGTCG
		R: GGGGTCATTGATGGCAACAATA
GAPDH	Mouse	F: TGCACCACCAACTGCTTAG
		R: GGATGCAGGGATGATGTTC

qRT-PCR, quantitative real-time polymerase chain reaction; IL, interleukin; TNF-α, tumor necrosis factor-α; ZO-1, zonula occludens-1; JAK2, janus kinase 2; STAT3, signal transducer and activator of transcription 3; HIF-1α, hypoxia-inducible factor 1 alpha; GAPDH, glyceraldehyde-3-phosphate dehydrogenase.

Conversely, administration of G3-C12 produced a dose-dependent reduction in apoptotic cells, with the G3-C12-H group showing the most pronounced decrease in apoptosis ($p < 0.01$ or $p < 0.001$) (Fig. 3A,B). To further evaluate apoptosis, the activity levels of Caspase-3 and Caspase-9 in intestinal tissue homogenates was assessed. Compared with the Sham group, the IRI group exhibited a marked elevation in Caspase-3 and Caspase-9 activity ($p < 0.001$). Treatment

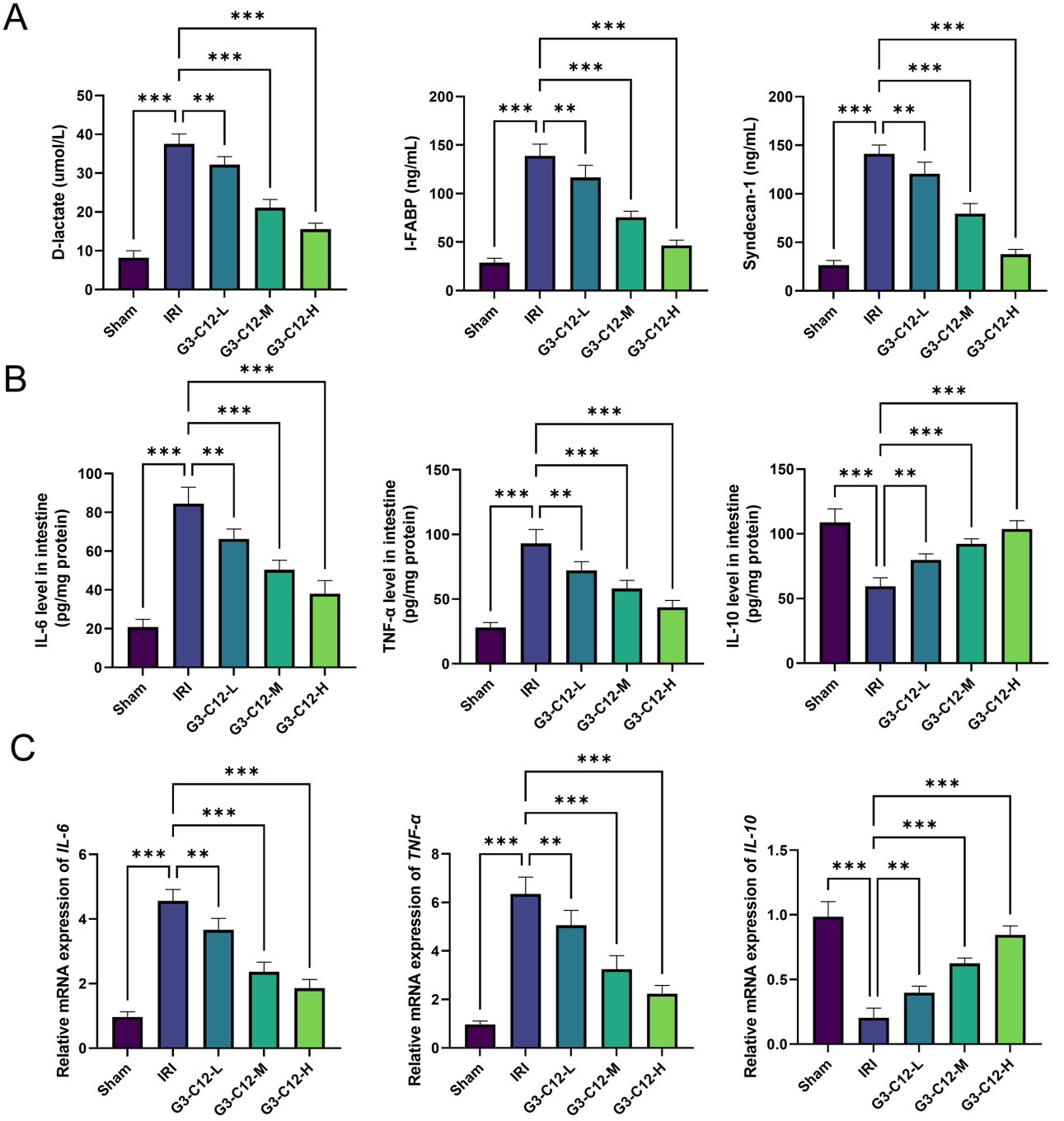

Fig. 1. Inhibition of Galectin-3 attenuates intestinal injury and inflammation in IRI mice. (A) Serum levels of D-Lactate, I-FABP, and Syndecan-1 were measured. (B) ELISA quantified IL-6, TNF-α, and IL-10 in intestinal homogenates. (C) qRT-PCR evaluated *IL-6*, *TNF-*α, and *IL-10* mRNA expression in intestinal tissue. n = 5; $^{**}p < 0.01$, $^{***}p < 0.001$ vs. IRI group. Sham, sham-operated control; G3-C12-L/M/H, low/medium/high doses of Galectin-3 inhibitor G3-C12; IRI, ischemia-reperfusion injury; I-FABP, intestinal fatty acid-binding protein; IL, interleukin; TNF-α, tumor necrosis factor-α; ELISA, enzyme-linked immunosorbent assay; qRT-PCR, quantitative real-time polymerase chain reaction.

with G3-C12 markedly reduced the activities of these caspases relative to the IRI group ($p < 0.01$ or $p < 0.001$), again displaying a dose-dependent trend (Fig. 3C). Collectively, these results demonstrate that Galectin-3 inhibition effectively attenuates IRI-induced intestinal epithelial apoptosis and suppresses the activation of apoptosis-related enzymes, thereby exerting a protective role against mucosal apoptotic injury.

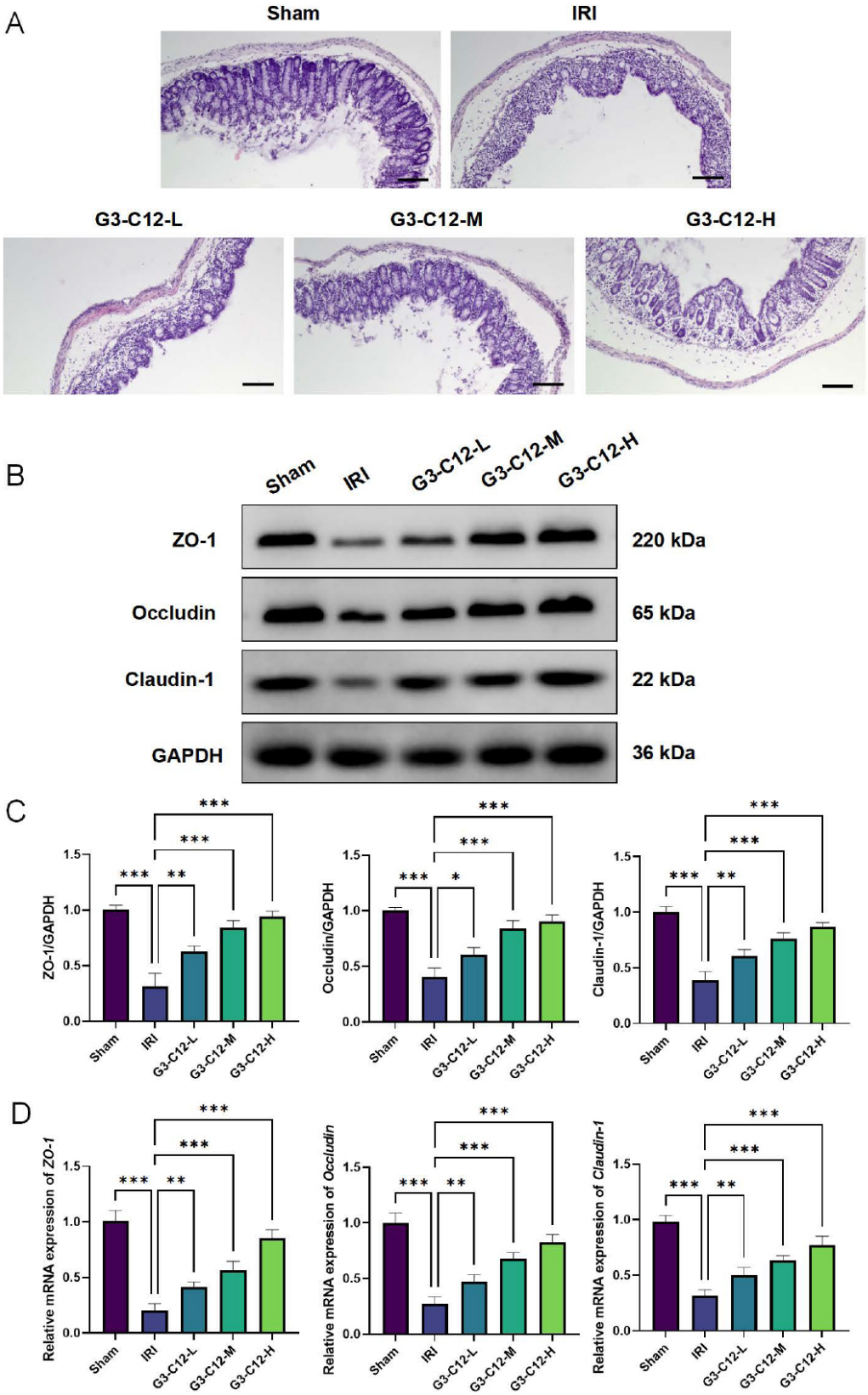

Fig. 2. Effects of Galectin-3 inhibitor on intestinal mucosal architecture and TJP expression in IRI mice. (A) H&E staining of intestinal tissue (magnification, 100×; scale bar = 100 μm). (B) WB analysis of ZO-1, occludin, and claudin-1 in intestinal tissue. (C) Densitometric quantification of protein levels. (D) qRT-PCR assessment of *ZO-1*, *occludin*, and *claudin-1* mRNA expression in intestinal tissue. n = 5; *$p < 0.05$, **$p < 0.01$, ***$p < 0.001$ vs. IRI group. TJP, tight junction protein; H&E, hematoxylin-eosin; WB, western blotting; ZO-1, zonula occludens-1; GAPDH, glyceraldehyde-3-phosphate dehydrogenase.

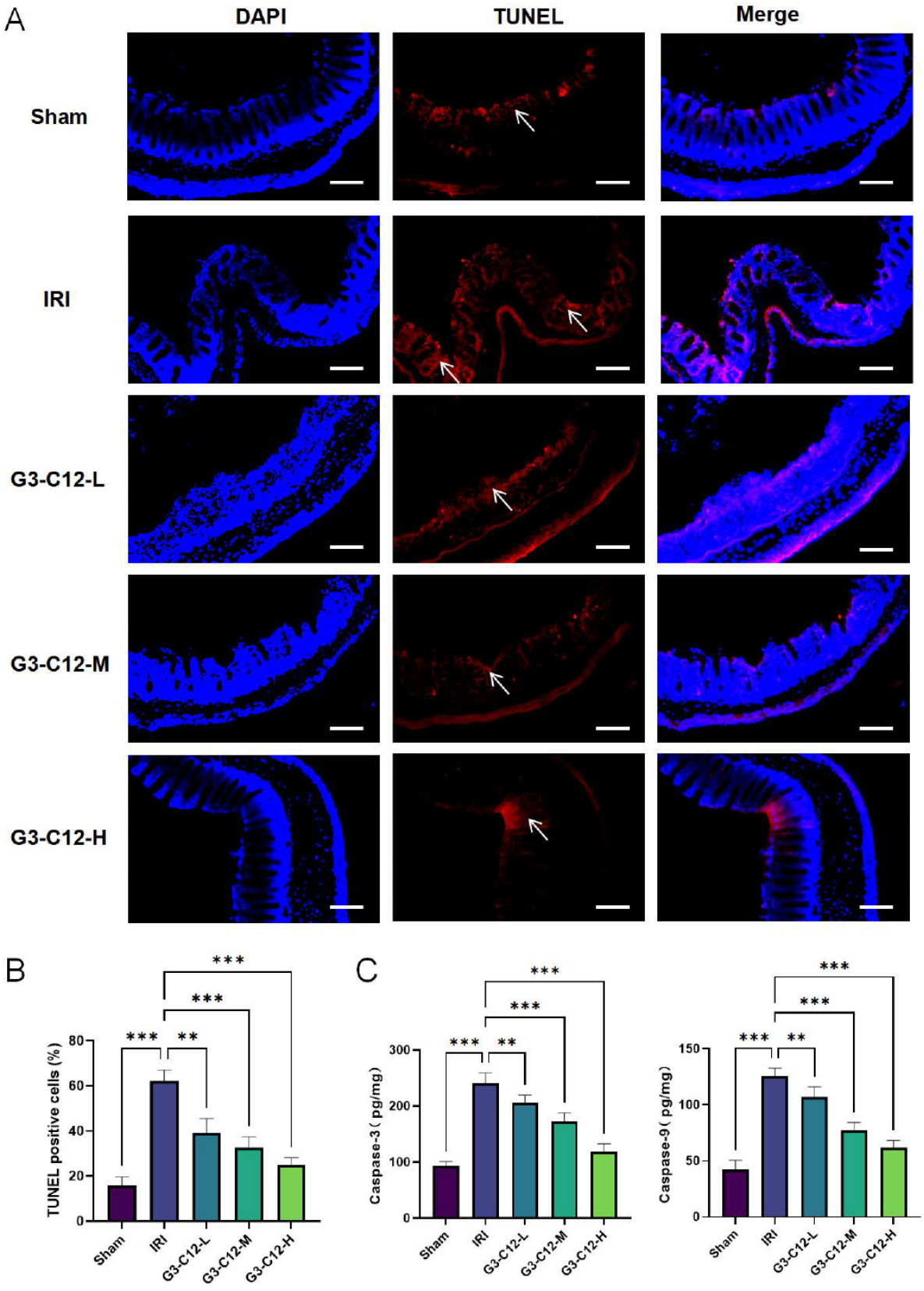

Fig. 3. Effects of Galectin-3 inhibition on intestinal epithelial cell apoptosis in IRI mice. (A) TUNEL staining in intestinal tissue (magnification, 100×; scale bar = 100 μm). (B) Quantification of TUNEL-positive cells. (C) Caspase-3 and Caspase-9 activities measured in intestinal tissue homogenates. n = 5; $^{**}p < 0.01$, $^{***}p < 0.001$ vs. IRI group. Note: The white arrow in (A) indicates typical apoptotic cells. TUNEL, terminal deoxynucleotidyl transferase dUTP nick-end labeling; DAPI, 4′6-diamidino-2-phenylindole.

Galectin-3 Inhibitor Attenuates IRI in Mice by Modulating the JAK2/STAT3 Signaling Pathway

To further investigate the mechanism by which Galectin-3 regulates the JAK2/STAT3 signaling pathway during IRI, we evaluated the expression of Galectin-3, JAK2, and STAT3 in intestinal tissues. Western blot analysis demonstrated that, relative to the Sham group, the IRI group had significantly elevated protein levels of Galectin-3, p-JAK2, and p-STAT3 ($p < 0.001$), indicating activation of the JAK2/STAT3 signaling pathway and upregulation of Galectin-3 following IRI. Treatment with the Galectin-3 inhibitor G3-C12 resulted in a dose-dependent decrease in Galectin-3, p-JAK2, and p-STAT3, with maximal inhibition in the G3-C12-H group ($p < 0.01$ or $p < 0.001$) (Fig. 4A,B). In contrast, total JAK2 and STAT3 expression remained unchanged across all groups. qRT-PCR analysis further confirmed these findings, showing consistent changes at the mRNA level ($p < 0.01$ or $p < 0.001$, Fig. 4C). Overall, these findings suggest that Galectin-3 acts as a key regulator in IRI, enhancing JAK2 phosphorylation via upstream signaling pathways, which contributes to intestinal inflammation and barrier dysfunction.

Galectin-3 Inhibitor Alleviates OGD/R-Induced Injury in Caco-2 Cells and Modulates Inflammatory Cytokine Expression

To determine the optimal intervention concentration of the Galectin-3 inhibitor G3-C12, a CCK-8 assay was performed to evaluate its effect on Caco-2 cell viability. Results showed that G3-C12 exhibited no significant cytotoxicity within the range of 0–50 μM, with all concentrations below 50 μM considered safe. However, at 75 μM, cell viability was significantly reduced ($p < 0.001$) (Fig. 5A). Under OGD/R conditions, G3-C12 at 10, 25, and 50 μM significantly improved cell viability, with 50 μM showing the strongest effect ($p < 0.05$ or $p < 0.001$) (Fig. 5B). Therefore, 50 μM was selected for subsequent experiments.

To validate the regulatory effect of the JAK2 agonist C-A1 on JAK2 expression, WB and qRT-PCR analyses were performed across treatment groups. Both JAK2 protein and mRNA levels were significantly upregulated in the C-A1-treated group compared to controls ($p < 0.001$) (Fig. 5C,D). These findings confirm that C-A1 effectively activates the JAK2 pathway, thereby providing a foundation for further investigation into Galectin-3 regulation of the JAK2/STAT3 axis. To confirm the successful establishment of the OGD/R model in Caco-2 cells, HIF-1α expression, a key hypoxia-responsive transcription factor, was assessed. WB results demonstrated a marked elevation of HIF-1α protein in the OGD/R group compared to controls, with quantitative analysis confirming statistical significance ($p < 0.001$) (Fig. 5E). Additionally, qRT-PCR results (Fig. 5F) were consistent with the Western blot findings, further supporting successful OGD/R model establishment in Caco-2 cells.

CCK-8 and LDH assays revealed that OGD/R treatment significantly reduced Caco-2 cell viability and enhanced LDH release relative to controls ($p < 0.001$), indicating enhanced cellular injury. Treatment with G3-C12 significantly improved cell viability and reduced LDH release ($p < 0.001$), while co-treatment with C-A1 partially reversed these protective effects ($p < 0.01$) (Fig. 5G,H). Cytokine analysis further revealed that OGD/R markedly enhanced the secretion of IL-6 and TNF-α into the supernatant while reducing IL-10 expression ($p < 0.001$) (Fig. 5I,J). G3-C12 intervention effectively suppressed IL-6 and TNF-α while enhancing IL-10 expression ($p < 0.01$ or $p < 0.001$). Co-treatment with C-A1, however, elevated IL-6 and TNF-α levels while decreasing IL-10 expression ($p < 0.01$ or $p < 0.001$) (Fig. 5I,J). Since C-A1 activates the JAK2/STAT3 pathway, these findings suggest that Galectin-3 inhibition-mediated suppression of JAK2/STAT3 contributes to IL-10 upregulation, whereas C-A1 counteracts the anti-inflammatory effect associated with G3-C12 by restoring pathway activity. Consistent results from qRT-PCR and ELISA analyses confirm that Galectin-3 inhibition alleviates OGD/R-induced cellular injury and contributes to anti-inflammatory activity.

Galectin-3 Inhibitor Attenuates OGD/R-Induced Apoptosis in Caco-2 Cells

TUNEL staining revealed a notable increase in apoptotic cells in the OGD/R group relative to controls ($p < 0.001$), suggesting that OGD/R strongly induces apoptosis. Treatment with G3-C12 significantly reduced apoptotic cell numbers ($p < 0.001$), while co-treatment with C-A1 significantly increased apoptosis relative to the G3-C12 group ($p < 0.001$), suggesting that C-A1 partially counteracted the anti-apoptotic effect of G3-C12 (Fig. 6A,B). Consistently, caspase activity assays showed that OGD/R treatment significantly enhanced Caspase-3 and Caspase-9 activity compared to controls ($p < 0.001$), while G3-C12 treatment markedly suppressed their activity ($p < 0.001$). Co-administration of C-A1, however, led to increased caspase activity relative to the G3-C12 group ($p < 0.01$) (Fig. 6C). Collectively, these findings demonstrate that G3-C12, a Galectin-3 inhibitor, effectively reduces OGD/R-induced apoptosis in Caco-2 cells.

Galectin-3 Inhibitor Enhances the Expression of TJPs and Restores Epithelial Barrier Function in OGD/R-Induced Injury

To evaluate the influence of Galectin-3 inhibitor on barrier function in Caco-2 cells subjected to OGD/R, the expression of TJP was analyzed by WB and qRT-PCR. WB analysis revealed a significant decrease in the protein expression of ZO-1, occludin, and claudin-1 in the OGD/R group compared to the Control group ($p < 0.001$), suggesting disruption of intercellular tight junction integrity. Treatment with G3-C12 markedly restored the expression

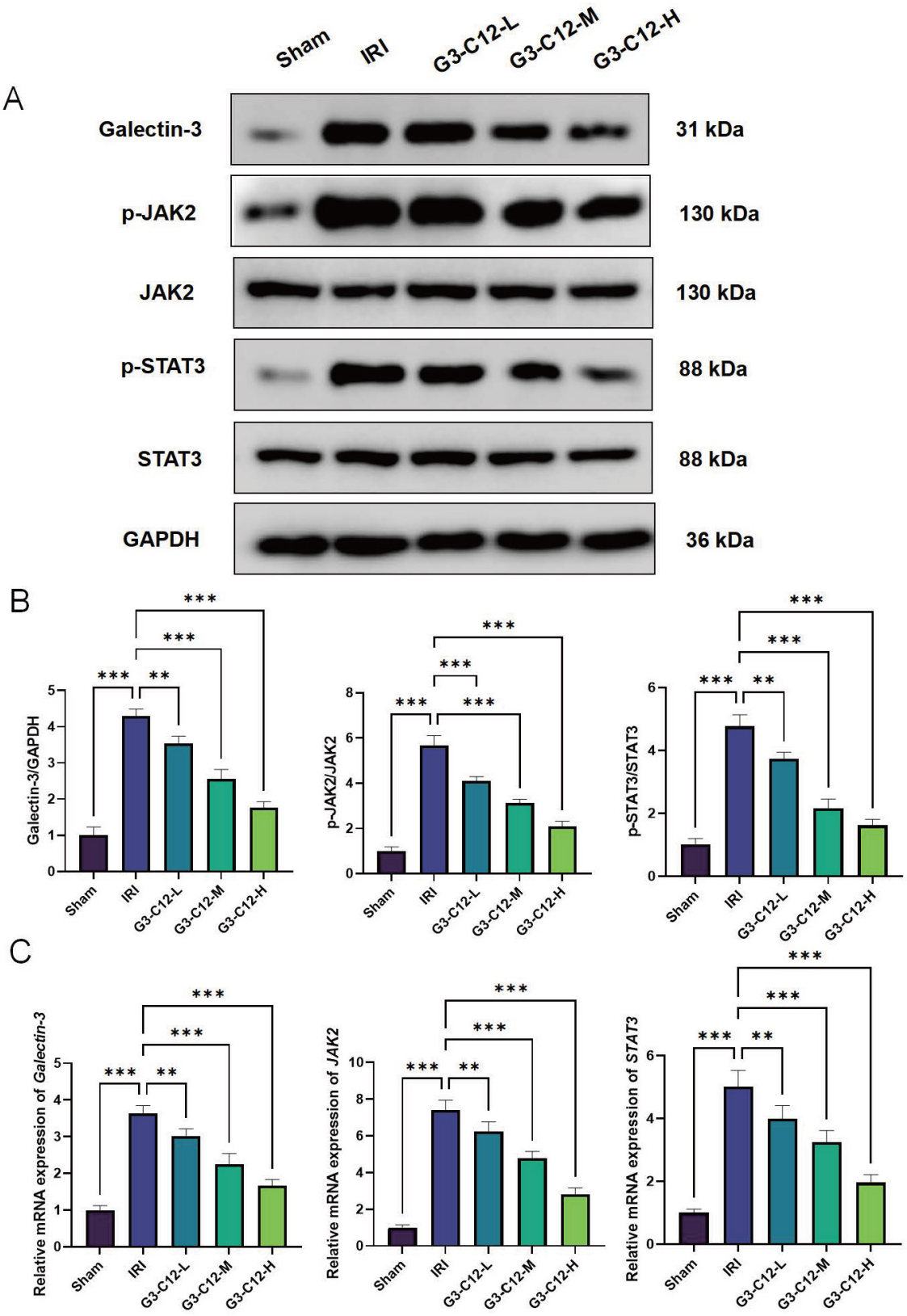

Fig. 4. Effects of Galectin-3 inhibition on Galectin-3 expression and JAK2/STAT3 signaling pathway in intestinal tissues of IRI mice. (A) WB analysis of Galectin-3 and JAK2/STAT3 pathway-related proteins in intestinal tissue. (B) Densitometric quantification of protein expression levels. (C) qRT-PCR analysis of *Galectin-3*, *JAK2*, and *STAT3* mRNA levels. n = 5; $^{**}p < 0.01$, $^{***}p < 0.001$ vs. IRI group. JAK2, janus kinase 2; STAT3, signal transducer and activator of transcription 3; p-JAK2, phosphorylated JAK2; p-STAT3, phosphorylated STAT3.

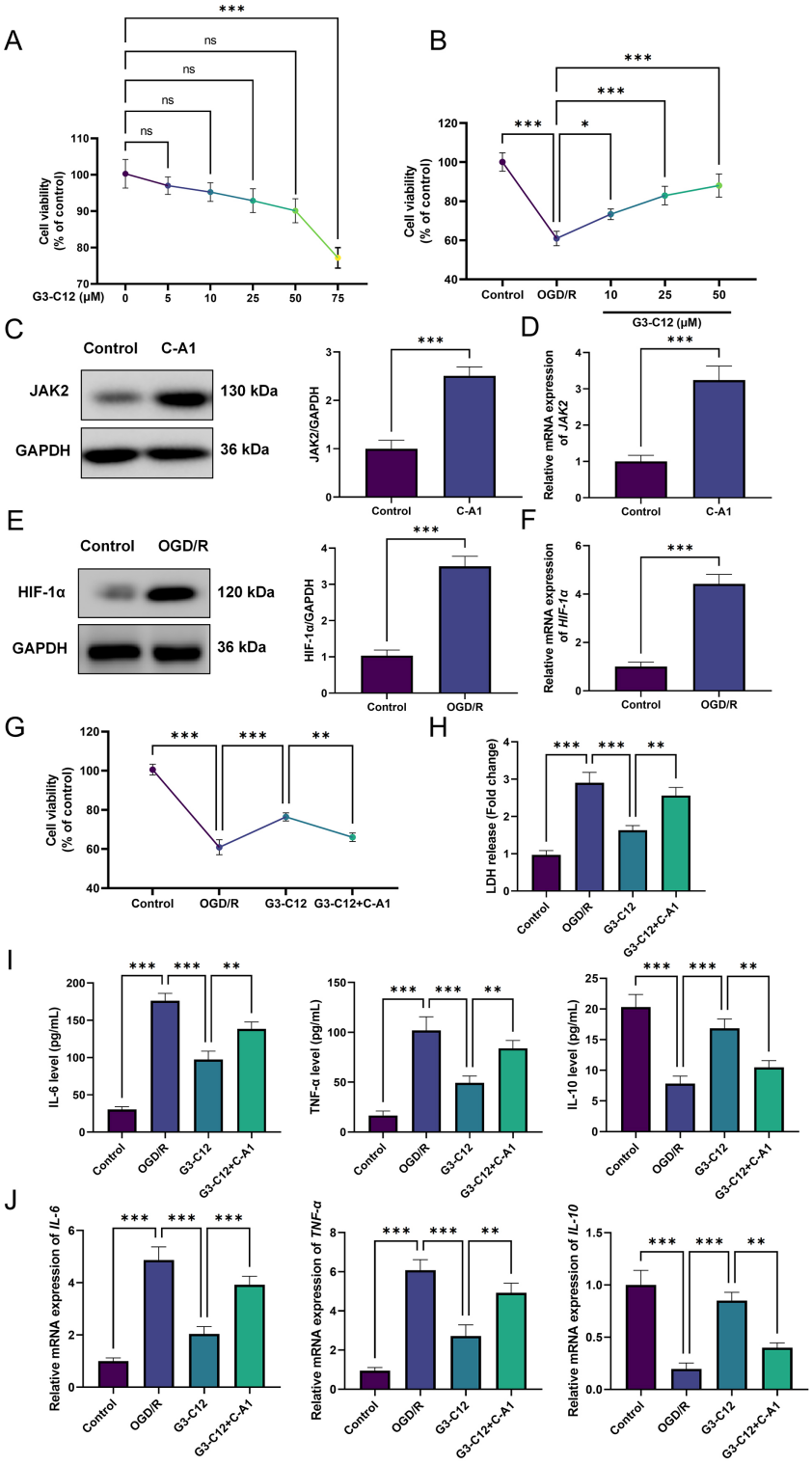

Fig. 5. Effects of Galectin-3 inhibition on OGD/R-induced cellular injury and inflammatory cytokine expression in Caco-2 cells. (A) Determination of the optimal G3-C12 concentration. (B) Cell viability under different treatment conditions. (C) WB analysis of JAK2 protein expression. (D) qRT-PCR analysis of *JAK2* mRNA expression. (E) WB analysis of HIF-1α protein expression. (F) qRT-PCR analysis of *HIF-1*α mRNA expression. (G) Cell viability assay. (H) LDH release assay. (I) ELISA measurement of IL-6, TNF-α, and IL-10 levels. (J) qRT-PCR analysis of *IL-6*, *TNF-*α, and *IL-10* mRNA expression. n = 3; ns: not significant, *$p < 0.05$, **$p < 0.01$, ***$p < 0.001$ vs. OGD/R group; **$p < 0.01$, ***$p < 0.001$ vs. G3-C12 group. HIF-1α, hypoxia-inducible factor 1 alpha; OGD/R, oxygen-glucose deprivation/reoxygenation; LDH, lactate dehydrogenase; C-A1, JAK2 agonist coumermycin A1; G3-C12, Galectin-3 inhibitor G3-C12; G3-C12 + C-A1, Galectin-3 inhibitor G3-C12 combined with JAK2 agonist C-A1.

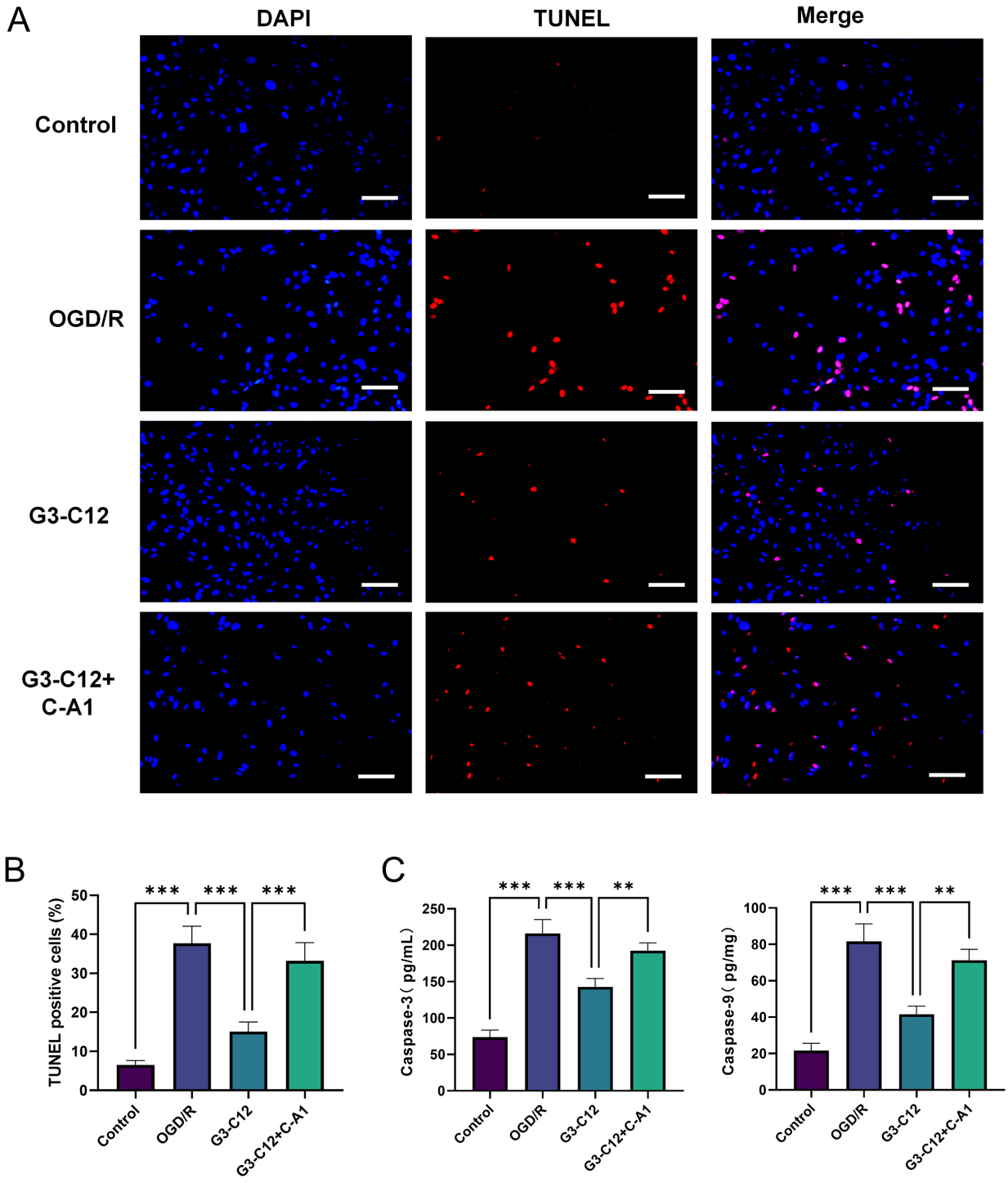

Fig. 6. Galectin-3 inhibition attenuates OGD/R-induced apoptosis in Caco-2 cells. (A) TUNEL staining of apoptotic cells (magnification, 200×; scale bar = 50 µm). (B) Quantification of TUNEL-positive apoptotic cells. (C) Caspase-3 and Caspase-9 enzymatic activities across groups. n = 3; ***$p < 0.001$ vs. OGD/R group; **$p < 0.01$, ***$p < 0.001$ vs. G3-C12 group.

of these TJPs ($p < 0.01$ or $p < 0.001$). However, co-administration of C-A1 markedly decreased their expression, partially offsetting the protective effects of G3-C12 ($p < 0.01$) (Fig. 7A,B). Consistently, qRT-PCR analysis revealed similar trends at the mRNA level (Fig. 7C). Collectively, these findings indicate that the Galectin-3 inhibitor G3-C12 effectively restores the expression of TJPs and improves barrier function in OGD/R-induced Caco-2 cells, whereas activation of the JAK2 pathway by C-A1 partially attenuates this protective effect.

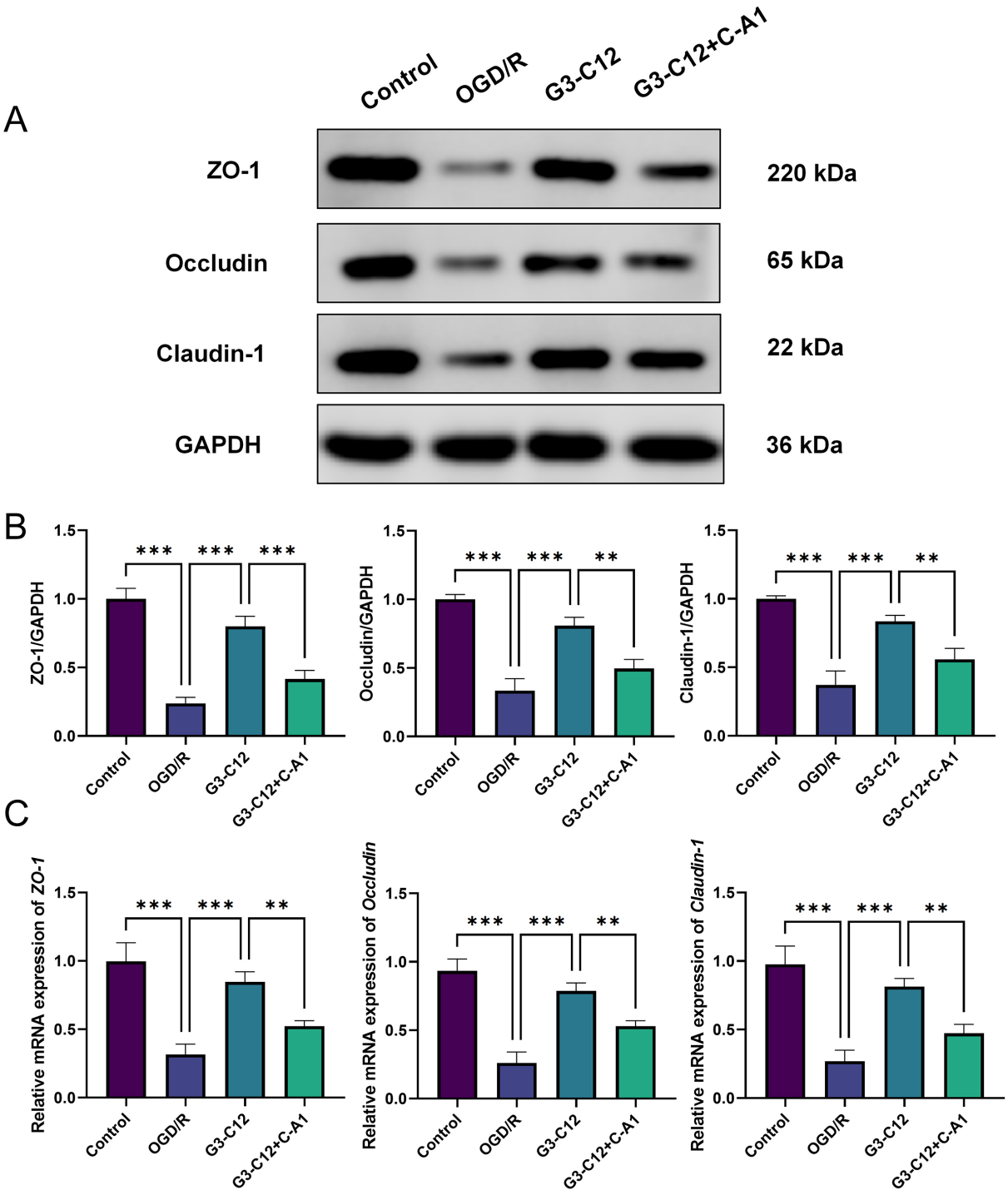

Fig. 7. Effects of Galectin-3 inhibition on TJPs in OGD/R-treated Caco-2 cells. (A) WB analysis of ZO-1, occludin, and claudin-1 expression. (B) Densitometric quantification of protein levels. (C) qRT-PCR analysis of TJPs mRNA levels. n = 3; ***$p < 0.001$ vs. OGD/R group; **$p < 0.01$, ***$p < 0.001$ vs. G3-C12 group.

Galectin-3 Inhibitor Mitigates OGD/R-Induced Cellular Injury by Modulating the JAK2/STAT3 Signaling Pathway

To further investigate the regulatory role of Galectin-3 on the JAK2/STAT3 signaling pathway, the expression of Galectin-3 and key signaling components was assessed by WB and qRT-PCR across treatment groups. WB analysis revealed that, compared to the Control group, OGD/R stimulation markedly elevated Galectin-3 expression, along with significant upregulation of p-JAK2 and p-STAT3 ($p < 0.001$), indicating that OGD/R activates both Galectin-3 and the JAK2/STAT3 signaling pathway. Administra-

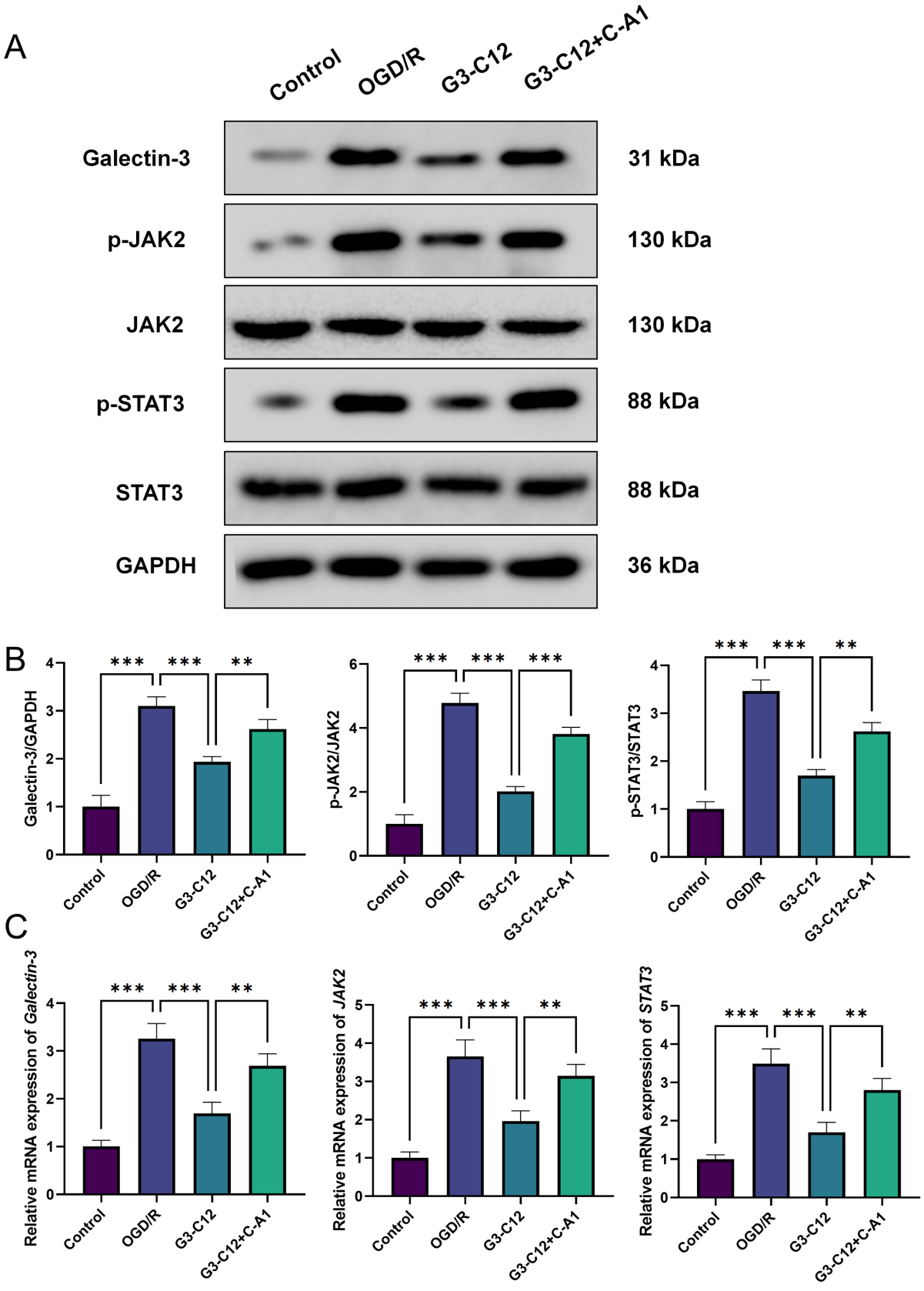

Fig. 8. Effects of Galectin-3 inhibition on JAK2/STAT3 signaling in OGD/R-treated Caco-2 cells. (A) WB analysis of Galectin-3, JAK2, and STAT3 proteins. (B) Densitometric quantification of protein expression. (C) qRT-PCR analysis of *Galectin-3*, *JAK2*, and *STAT3* mRNA expression. n = 3; ***$p < 0.001$ vs. OGD/R group; **$p < 0.01$, ***$p < 0.001$ vs. G3-C12 group.

tion of the G3-C12 significantly suppressed the OGD/R-induced increase in Galectin-3 and reduced phosphorylation of JAK2 and STAT3 ($p < 0.01$ or $p < 0.001$), suggesting that G3-C12 effectively blocks the activation of the JAK2/STAT3 pathway downstream of Galectin-3 signaling. However, co-treatment with C-A1 restored p-JAK2 and p-STAT3 expression, partially reversing the inhibitory effects of G3-C12 ($p < 0.01$) (Fig. 8A,B). qRT-PCR findings aligned with the observed protein expression profiles (Fig. 8C). The findings indicate that Galectin-3 may indirectly promote activation of the JAK2/STAT3 signaling pathway via upstream regulators, thus mediating protective effects in intestinal epithelial cells under hypoxia/reoxygenation stress.

Discussion

IRI is a common and severe clinical condition frequently observed in abdominal and thoracic vascular surgeries as well as small bowel transplantation [1]. It involves alternating interruptions and restorations of intestinal blood flow, leading to mucosal structural damage, barrier dysfunction, and the activation of inflammatory cascades, oxidative stress, and apoptosis, which may progress to SIRS and MODS [22–24]. This study investigated the cytoprotective role of Galectin-3 in regulating the JAK2/STAT3 signaling pathway amid intestinal epithelial barrier disruption in a mouse IRI model. Galectin-3 has been implicated in multiple organ IRI models, influencing cellular adhesion, migration, apoptosis, and inflammation. Previous studies reported elevated Galectin-3 levels in cardiac and renal IR injury models, where it contributed to tissue damage via downstream signaling pathways [25,26].

Inflammation and apoptosis are central mechanisms underlying intestinal injury during IRI. In the early phase of reperfusion, rapid activation of innate immunity leads to excessive release of pro-inflammatory cytokines (e.g., TNF-α, IL-6), while accumulation of reactive oxygen species (ROS) induces intracellular damage and signaling dysregulation [27]. These inflammatory responses aggravate local mucosal injury and promote bacterial translocation and endotoxemia, thereby initiating inflammation in distant organs [28,29]. Apoptosis, primarily mediated through caspase-dependent pathways, causes loss of intestinal epithelial cells, further impairing mucosal integrity and amplifying inflammation, creating a vicious cycle [30]. Administration of a Galectin-3 inhibitor markedly reduced cytokine production and apoptosis, demonstrating dual anti-inflammatory and anti-apoptotic properties in IRI. These findings are consistent with previous reports that Galectin-3 inhibition alleviates tissue damage by suppressing both inflammation and apoptosis [20,25].

Earlier studies have demonstrated that the JAK2/STAT3 signaling axis is a crucial intracellular transduction pathway regulating inflammation, apoptosis, and tissue repair [31,32]. It is activated in several organ IR injury models. For example, myocardial IR injury involves JAK2/STAT3 activation, which upregulates IL-6 and TNF-α expression and aggravates tissue damage [33], while inhibition of this pathway reduces inflammation and cell death in hepatic and renal IR injury, thereby preserving organ function [34,35]. Pro-inflammatory stimuli induce JAK2 phosphorylation, leading to STAT3 activation. Phosphorylated STAT3 subsequently translocate into the nucleus and regulates inflammation- and apoptosis-related genes such as IL-6 and Caspase-3 [36,37]. Our findings demonstrated that Galectin-3 serves as an upstream regulator of the JAK2/STAT3 pathway in intestinal IRI, linking Galectin-3 activity with IR-induced tissue injury. In the mouse model, Galectin-3, p-JAK2, and p-STAT3 levels were significantly elevated, whereas treatment with the Galectin-3 inhibitor G3-C12 reduced these proteins in a dose-dependent manner. These observations reinforce the role of Galectin-3 in JAK2/STAT3 activation and highlight its therapeutic potential to alleviate IRI-related inflammation and barrier dysfunction.

The integrity of the intestinal mucosal barrier depends on TJPs, including ZO-1, occludin, and claudin-1 [38–40]. ZO-1 links membrane proteins to the cytoskeleton, maintaining polarity and barrier stability [41], while occludin and claudins regulate paracellular permeability [42]. IRI-associated inflammation and ROS reduce TJP expression and disrupt their distribution, leading to epithelial barrier breakdown, increased permeability, and systemic inflammation [23]. In our study, histological analysis revealed significant mucosal shedding, edema, and inflammation in IRI mouse intestines. WB and qRT-PCR confirmed marked downregulation of TJPs, which was reversed by Galectin-3 inhibition. These findings suggest that Galectin-3 inhibition preserves tight junction integrity, likely through attenuation of inflammation and apoptosis. Previous studies have shown that excessive STAT3 activation suppresses TJP expression [43–45], especially claudin-1 [46], providing a mechanistic basis for our findings and suggesting that Galectin-3 inhibition may restore barrier function by modulating both inflammatory and structural pathways.

An *in vitro* Caco-2 cell model subjected to OGD/R was employed to mimic ischemia-reperfusion injury. Treatment with Galectin-3 inhibitor G3-C12 improved cell viability, reduced LDH release, and attenuated inflammation and apoptosis. It also restored TJP expression and suppressed overactivation of Galectin-3 and JAK2/STAT3 signaling, as evidenced by reduced phosphorylation of JAK2 and STAT3. Co-treatment with the JAK2 agonist C-A1 partially reversed the protective effects of G3-C12. These outcomes confirm at the cellular level that Galectin-3 regulates inflammation, apoptosis, and epithelial barrier integrity via JAK2/STAT3 modulation, supporting our *in vivo* findings and further strengthening its potential as a therapeutic target in IRI.

This study systematically elucidates the critical role of Galectin-3 in the pathogenesis of IRI: by activating the JAK2/STAT3 signaling pathway, Galectin-3 mediates amplification of inflammation, promotes apoptosis, and disrupts the epithelial barrier. Inhibition of Galectin-3 effectively alleviates these pathological damages, reduces mucosal injury, and restores barrier integrity, providing a potential therapeutic target for IRI. However, this study has several limitations. First, Galectin-3 knockout or overexpression models were not employed to further validate its mechanistic role. Second, the systemic effects and long-term safety of Galectin-3 inhibition *in vivo* remain unclear. Future research should investigate Galectin-3 expression levels in tissues from IRI patients and assess their correlation with disease severity to further establish its potential as a therapeutic target or diagnostic biomarker.

Conclusion

This study demonstrates that Galectin-3 contributes to inflammation, apoptosis, and intestinal mucosal barrier disruption during IRI through activation of the JAK2/STAT3 signaling pathway. Inhibition of Galectin-3 significantly attenuates inflammatory responses, suppresses apoptosis, and upregulates the expression of TJPs, thereby preserving barrier integrity. Collectively, these findings highlight Galectin-3 as a promising target for the development of novel therapeutic strategies against IRI.

Availability of Data and Materials

The analyzed data sets generated during the study are available from the corresponding author upon reasonable request.

Author Contributions

WY and ZL conceptualized and designed the study; LX, QC, SX, WY, and ZL performed the research. LX, QC, SX, WY, and ZL contributed to data acquisition. WY and ZL analyzed and interpreted data for the work. LX, QC, and ZL provided help and advice on the research study. WY and ZL have been involved in drafting the manuscript, and all authors have been involved in revising it critically for important intellectual content. All authors contributed to important editorial changes in the manuscript. All authors read and approved the final manuscript. All authors have participated sufficiently in the work and agreed to be accountable for all aspects of the work.

Ethics Approval and Consent to Participate

All animal experiments were approved by the Experimental Animal Center of Wenzhou University (Approval No. WZU-2022-057). All procedures were carried out in accordance with institutional ethical guidelines, with efforts made to minimize animal use and suffering.

Acknowledgment

Not applicable.

Funding

This research was funded by the Science and Technology Program of Wenzhou (No. Y20240249).

Conflict of Interest

The authors declare no conflict of interest.

References

[1] Jin B, Li G, Zhou L, Fan Z. Mechanism Involved in Acute Liver Injury Induced by Intestinal Ischemia-Reperfusion. Frontiers in Pharmacology. 2022; 13: 924695. https://doi.org/10.3389/fphar.2022.924695.

[2] Shen X, Shi H, Chen X, Han J, Liu H, Yang J, *et al*. Esculetin Alleviates Inflammation, Oxidative Stress and Apoptosis in Intestinal Ischemia/Reperfusion Injury via Targeting SIRT3/AMPK/mTOR Signaling and Regulating Autophagy. Journal of Inflammation Research. 2023; 16: 3655–3667. https://doi.org/10.2147/JIR.S413941.

[3] Sheng R, Wang W, Zeng W, Li B, Yu H, Li X, *et al*. Macrophage Membrane Coated Manganese Dioxide Nanoparticles Loaded with Rapamycin Alleviate Intestinal Ischemia-Reperfusion Injury by Reducing Oxidative Stress and Enhancing Autophagy. International Journal of Nanomedicine. 2025; 20: 3541–3557. https://doi.org/10.2147/IJN.S507546.

[4] Assimakopoulos SF, Eleftheriotis G, Lagadinou M, Karamouzos V, Dousdampanis P, Siakallis G, *et al*. SARS CoV-2-Induced Viral Sepsis: The Role of Gut Barrier Dysfunction. Microorganisms. 2022; 10: 1050. https://doi.org/10.3390/microorganisms10051050.

[5] Liao S, Luo J, Kadier T, Ding K, Chen R, Meng Q. Mitochondrial DNA Release Contributes to Intestinal Ischemia/Reperfusion Injury. Frontiers in Pharmacology. 2022; 13: 854994. https://doi.org/10.3389/fphar.2022.854994.

[6] Hao W, Cha R, Wang M, Zhang P, Jiang X. Impact of nanomaterials on the intestinal mucosal barrier and its application in treating intestinal diseases. Nanoscale Horizons. 2021; 7: 6–30. https://doi.org/10.1039/d1nh00315a.

[7] An J, Liu Y, Wang Y, Fan R, Hu X, Zhang F, *et al*. The Role of Intestinal Mucosal Barrier in Autoimmune Disease: A Potential Target. Frontiers in Immunology. 2022; 13: 871713. https://doi.org/10.3389/fimmu.2022.871713.

[8] Chen S, He R, He B, Xu L, Zhang S. Potential Roles of Exosomal lncRNAs in the Intestinal Mucosal Immune Barrier. Journal of Immunology Research. 2021; 2021: 7183136. https://doi.org/10.1155/2021/7183136.

[9] Sari SM, Teng YY, Wang CH, Kuo C, Hsu BG. MO687: Positive Association of Serum Galectin-3 Level with the Peripheral Arterial Disease in Patients with Peritoneal Dialysis. Nephrology Dialysis Transplantation. 2022; 37. https://doi.org/10.1093/ndt/gfac078.024.

[10] Zhou Y, Qiu T, Wang T, Yu B, Xia K, Guo J, *et al*. Research progress on the role of mitochondria in the process of hepatic ischemia-reperfusion injury. Gastroenterology Report. 2024; 12: goae066. https://doi.org/10.1093/gastro/goae066.

[11] Song Z, Zhong X, Ning Z, Song X. The Protective Effect of miR-27-3p on Ischemia-Reperfusion-Induced Myocardial Injury Depends on HIF-1α and Galectin-3. Journal of Cardiovascular

Translational Research. 2022; 15: 772–785. https://doi.org/10.1007/s12265-021-10203-y.

[12] Sun H, Peng J, Cai S, Nie Q, Li T, Kellum JA, *et al*. A translational study of Galectin-3 as an early biomarker and potential therapeutic target for ischemic-reperfusion induced acute kidney injury. Journal of Critical Care. 2021; 65: 192–199. https://doi.org/10.1016/j.jcrc.2021.06.013.

[13] Wang JY, Lu PH, Lin WW, Wei YH, Chiu LY, Chern SR, *et al*. Galectin-3 regulates UVB-induced inflammation in skin. Journal of Dermatological Science. 2020; 98: 119–127. https://doi.org/10.1016/j.jdermsci.2020.03.007.

[14] Drennan AC, Rui L. HiJAKing the epigenome in leukemia and lymphoma. Leukemia & Lymphoma. 2017; 58: 2540–2547. https://doi.org/10.1080/10428194.2017.1312370.

[15] Raychaudhuri SP, Raychaudhuri SK. JAK inhibitor: Introduction. Indian Journal of Dermatology, Venereology and Leprology. 2023; 89: 688–690. https://doi.org/10.25259/IJDVL_8_2023.

[16] Song T, Zhang Y, Zhu L, Zhang Y, Song J. The role of JAK/STAT signaling pathway in cerebral ischemia-reperfusion injury and the therapeutic effect of traditional Chinese medicine: A narrative review. Medicine. 2023; 102: e35890. https://doi.org/10.1097/MD.0000000000035890.

[17] Zhang M, Zhang Y, Peng J, Huang Y, Gong Z, Lu H, *et al*. Gastrodin against oxidative stress-inflammation crosstalk via inhibiting mtDNA/TLR9 and JAK2/STAT3 signaling to ameliorate ischemic stroke injury. International Immunopharmacology. 2024; 141: 113012. https://doi.org/10.1016/j.intimp.2024.113012.

[18] Yang B, Zang LE, Cui JW, Zhang MY, Ma X, Wei LL. Melatonin Plays a Protective Role by Regulating miR-26a-5p-NRSF and JAK2-STAT3 Pathway to Improve Autophagy, Inflammation and Oxidative Stress of Cerebral Ischemia-Reperfusion Injury. Drug Design, Development and Therapy. 2020; 14: 3177–3188. https://doi.org/10.2147/DDDT.S262121.

[19] Zundler S, Neurath MF. Integrating Immunologic Signaling Networks: The JAK/STAT Pathway in Colitis and Colitis-Associated Cancer. Vaccines. 2016; 4: 5. https://doi.org/10.3390/vaccines4010005.

[20] Mo D, Tian W, Zhang HN, Feng YD, Sun Y, Quan W, *et al*. Cardioprotective effects of galectin-3 inhibition against ischemia/reperfusion injury. European Journal of Pharmacology. 2019; 863: 172701. https://doi.org/10.1016/j.ejphar.2019.172701.

[21] Liu Y, Ji T, Jiang H, Chen M, Liu W, Zhang Z, *et al*. Emodin alleviates intestinal ischemia-reperfusion injury through antioxidant stress, anti-inflammatory responses and anti-apoptosis effects via Akt-mediated HO-1 upregulation. Journal of Inflammation. 2024; 21: 25. https://doi.org/10.1186/s12950-024-00392-z.

[22] Liu M, Wen H, Zuo L, Song X, Geng Z, Ge S, *et al*. Bryostatin-1 attenuates intestinal ischemia/reperfusion-induced intestinal barrier dysfunction, inflammation, and oxidative stress via activation of Nrf2/HO-1 signaling. FASEB Journal. 2023; 37: e22948. https://doi.org/10.1096/fj.202201540R.

[23] Li G, Wang S, Fan Z. Oxidative Stress in Intestinal Ischemia-Reperfusion. Frontiers in Medicine. 2022; 8: 750731. https://doi.org/10.3389/fmed.2021.750731.

[24] Zhang M, Liu Q, Meng H, Duan H, Liu X, Wu J, *et al*. Ischemia-reperfusion injury: molecular mechanisms and therapeutic targets. Signal Transduction and Targeted Therapy. 2024; 9: 12. https://doi.org/10.1038/s41392-023-01688-x.

[25] Zhang M, Cheng K, Chen H, Tu J, Shen Y, Pang L, *et al*. Galectin-3 knock down inhibits cardiac ischemia-reperfusion injury through interacting with bcl-2 and modulating cell apoptosis. Archives of Biochemistry and Biophysics. 2020; 694: 108602. https://doi.org/10.1016/j.abb.2020.108602.

[26] Hassan FE, Aboulhoda BE, Ali IH, Elwi HM, Matter LM, Abdallah HA, *et al*. Evaluating the protective role of trimetazidine versus nano-trimetazidine in amelioration of bilateral renal ischemia/reperfusion induced neuro-degeneration: Implications of ERK1/2, JNK and Galectin-3 /NF-κB/TNF-α/HMGB-1 signaling. Tissue & Cell. 2023; 85: 102241. https://doi.org/10.1016/j.tice.2023.102241.

[27] Zhu Y, Li J, Zhang P, Peng B, Li C, Ming Y, *et al*. Berberine protects hepatocyte from hypoxia/reoxygenation-induced injury through inhibiting circDNTTIP2. PeerJ. 2023; 11: e16080. https://doi.org/10.7717/peerj.16080.

[28] Canovai E, Farré R, De Hertogh G, Dubois A, Vanuytsel T, Pirenne J, *et al*. Tranilast Reduces Intestinal Ischemia Reperfusion Injury in Rats Through the Upregulation of Heme-Oxygenase (HO)-1. Journal of Clinical Medicine. 2025; 14: 3254. https://doi.org/10.3390/jcm14093254.

[29] Elimam H, Gauvin J, Huynh DN, Ménard L, Al-Hawat ML, Harb D, *et al*. Targeting CD36 With EP 80317 Reduces Remote Inflammatory Response to Hind Limb Ischemia-Reperfusion in Mice. Journal of Biochemical and Molecular Toxicology. 2024; 38: e70057. https://doi.org/10.1002/jbt.70057.

[30] Blander JM. On cell death in the intestinal epithelium and its impact on gut homeostasis. Current Opinion in Gastroenterology. 2018; 34: 413–419. https://doi.org/10.1097/MOG.0000000000000481.

[31] Mengie Ayele T, Tilahun Muche Z, Behaile Teklemariam A, Bogale Kassie A, Chekol Abebe E. Role of JAK2/STAT3 Signaling Pathway in the Tumorigenesis, Chemotherapy Resistance, and Treatment of Solid Tumors: A Systemic Review. Journal of Inflammation Research. 2022; 15: 1349–1364. https://doi.org/10.2147/JIR.S353489.

[32] Huang B, Lang X, Li X. The role of IL-6/JAK2/STAT3 signaling pathway in cancers. Frontiers in Oncology. 2022; 12: 1023177. https://doi.org/10.3389/fonc.2022.1023177.

[33] Liu S, Yang Y, Song YQ, Geng J, Chen QL. Protective effects of N(2) L alanyl L glutamine mediated by the JAK2/STAT3 signaling pathway on myocardial ischemia reperfusion. Molecular Medicine Reports. 2018; 17: 5102–5108. https://doi.org/10.3892/mmr.2018.8543.

[34] Zhang B, Su L, Chen Z, Wu M, Wei J, Lin Y. Exosomes derived from Baicalin-pretreated bone mesenchymal stem cells improve Th17/Treg imbalance after hepatic ischemia-reperfusion via FGF21 and the JAK2/STAT3 pathway. IUBMB Life. 2024; 76: 534–547. https://doi.org/10.1002/iub.2810.

[35] Zhao X, Zhang E, Ren X, Bai X, Wang D, Bai L, *et al*. Edaravone alleviates cell apoptosis and mitochondrial injury in ischemia-reperfusion-induced kidney injury via the JAK/STAT pathway. Biological Research. 2020; 53: 28. https://doi.org/10.1186/s40659-020-00297-0.

[36] Panda SP, Kesharwani A, Datta S, Prasanth DSNBK, Panda SK, Guru A. JAK2/STAT3 as a new potential target to manage neurodegenerative diseases: An interactive review. European Journal of Pharmacology. 2024; 970: 176490. https://doi.org/10.1016/j.ejphar.2024.176490.

[37] Hu Z, Sui Q, Jin X, Shan G, Huang Y, Yi Y, *et al*. IL6-STAT3-C/EBPβ-IL6 positive feedback loop in tumor-associated macrophages promotes the EMT and metastasis of lung adenocarcinoma. Journal of Experimental & Clinical Cancer Research: CR. 2024; 43: 63. https://doi.org/10.1186/s13046-024-02989-x.

[38] Xu CM, Li XM, Qin BZ, Liu B. Effect of tight junction protein of intestinal epithelium and permeability of colonic mucosa in pathogenesis of injured colonic barrier during chronic recovery stage of rats with inflammatory bowel disease. Asian Pacific Journal of Tropical Medicine. 2016; 9: 148–152. https:

//doi.org/10.1016/j.apjtm.2016.01.001.

[39] Neurath MF, Artis D, Becker C. The intestinal barrier: a pivotal role in health, inflammation, and cancer. The Lancet. Gastroenterology & Hepatology. 2025; 10: 573–592. https://doi.org/10.1016/S2468-1253(24)00390-X.

[40] Kaminsky LW, Al-Sadi R, Ma TY. IL-1β and the Intestinal Epithelial Tight Junction Barrier. Frontiers in Immunology. 2021; 12: 767456. https://doi.org/10.3389/fimmu.2021.767456.

[41] Utepbergenov DI, Fanning AS, Anderson JM. Dimerization of the scaffolding protein ZO-1 through the second PDZ domain. The Journal of Biological Chemistry. 2006; 281: 24671–24677. https://doi.org/10.1074/jbc.M512820200.

[42] Wei D, Xu M, Cui W, Feng X, Wei L, Wang K, *et al*. Research progress on the role of Claudin family proteins in mediating blood-brain barrier selective permeability in tumor metastasis. American Journal of Translational Research. 2025; 17: 2411–2421. https://doi.org/10.62347/GGGX3909.

[43] Zeng L, Wang Y, Shen J, Wei X, Wu Y, Chi X, *et al*. TIPE2 aggravates experimental colitis and disrupts intestinal epithelial barrier integrity by activating JAK2/STAT3/SOCS3 signal pathway. Experimental Cell Research. 2024; 443: 114287. https://doi.org/10.1016/j.yexcr.2024.114287.

[44] Bao X, Tang Y, Lv Y, Fu S, Yang L, Chen Y, *et al*. Tetrastigma hemsleyanum polysaccharide ameliorated ulcerative colitis by remodeling intestinal mucosal barrier function via regulating the SOCS1/JAK2/STAT3 pathway. International Immunopharmacology. 2024; 137: 112404. https://doi.org/10.1016/j.intimp.2024.112404.

[45] Hong ZS, Xie J, Wang XF, Dai JJ, Mao JY, Bai YY, *et al*. *Moringa oleifera* Lam. Peptide Remodels Intestinal Mucosal Barrier by Inhibiting JAK-STAT Activation and Modulating Gut Microbiota in Colitis. Frontiers in Immunology. 2022; 13: 924178. https://doi.org/10.3389/fimmu.2022.924178.

[46] Ryu WI, Lee H, Bae HC, Jeon J, Ryu HJ, Kim J, *et al*. IL-33 down-regulates CLDN1 expression through the ERK/STAT3 pathway in keratinocytes. Journal of Dermatological Science. 2018; 90: 313–322. https://doi.org/10.1016/j.jdermsci.2018.02.017.